Identification of Preoperative Language Tracts for Intrinsic Frontotemporal Diseases: A Pilot Reconstruction Algorithm in a Middle-Income Country

Edgar G. Ordóñez-Rubiano[1], Francisco A. Valderrama-Arias[1], Jonathan A. Forbes[2], Jason M. Johnson[3], Iyan Younus[4], Jorge H. Marín-Muñoz[5], Mariana Sánchez-Montaño[6], Diego A. Angulo[7,8], Hernando A. Cifuentes-Lobelo[1], William Cortes-Lozano[1], Maria C. Pedraza-Ciro[9], May Leonardo Bello-Dávila[10], Javier G. Patiño-Gómez[1], Edgar G. Ordóñez-Mora[1]

■ OBJECTIVE: **Diffusion tensor imaging (DTI) tractography provides useful information that can be used to optimize surgical planning and help avoid injury during subcortical dissection of eloquent tracts. The objective is to provide a safe, timely, and affordable algorithm for preoperative DTI language reconstruction for intrinsic frontotemporal diseases.**

■ METHODS: **We reviewed a prospectively acquired database of preoperative DTI reconstruction for resection of left frontotemporal lesions over 3 years at Hospital de San José and Hospital Infantil Universitario San José, Fundación Universitaria de Ciencias de la Salud, Bogota, Colombia. Preoperative and postoperative clinical and radiographic features were determined from retrospective chart review. A comprehensive review of the structural and functional anatomy of the language tracts was performed. Separate reconstruction of both ventral (semantic) and dorsal (phonologic) stream pathways is described: arcuate fasciculus, superior longitudinal fasciculus, inferior fronto-occipital fasciculus, uncinate fasciculus, and inferior longitudinal fasciculus.**

■ RESULTS: **Between January 2015 and January 2018, 44 tumor cases were found to be resected with preoperative fiber tracking planning and neuronavigation-guided surgery. Ten patients (7 women, 3 men) aged 28–65 years underwent resection of an intrinsic frontotemporal lesion with preoperative DTI tractography reconstruction of language tracts. Eight cases (80%) were high-grade gliomas and 2 (20%) were cavernous malformations. In 5 cases (50%), the lesion was in the frontal lobe and in 5 (50%), it was in the temporal lobe. The extent of resection was classified as gross total resection (100%), subtotal resection (>90%), or partial resection (<90%). Gross total resection was achieved in 5 cases (50%), subtotal resection was achieved in 4 cases (40%), and partial resection in the remaining case (10%). Compromised tracts included superior longitudinal fasciculus in 7 (70%), inferior longitudinal fasciculus in 4 (40%), the arcuate fasciculus in 3 (30%), and uncinate fasciculus in 1 (10%). Language function was unchanged or improved in 90% of patients. New-onset postoperative language decline occurred in 1 patient, who recovered transient phonemic paraphasias**

Key words
- Diffusion tensor imaging
- Language
- Temporal lobe
- Tractography
- White matter

Abbreviations and Acronyms
2D: Two-dimensional
3D: Three-dimensional
AF: Arcuate fasciculus
CNS: Central nervous system
DCS: Direct cortical stimulation
DSS: Direct subcortical stimulation
DTI: Diffusion tensor imaging
fMRI: Functional magnetic resonance imaging
FOV: Field of view
IFOF: Inferior fronto-occipital fasciculus
ILF: Inferior longitudinal fasciculus
LMIC: Low- to middle-income country
MRI: Magnetic resonance imaging
ROI: Region of interest
SLF: Superior longitudinal fasciculus
SLF-tp: Superior longitudinal fasciculus temporoparietal segment
TE: Echo time
TR: Repetition time

From the [1]Department of Neurological Surgery, Fundación Universitaria de Ciencias de la Salud, Hospital Infantil Universitario de San José, Bogotá, Colombia; [2]Department of Neurological Surgery, University of Cincinnati College of Medicine, Cincinnati, Ohio; [3]Neuroradiology, Department of Diagnostic Radiology, The University of Texas MD Anderson Cancer Center, Houston, Texas; [4]Weill Cornell Medical College, New York, New York, USA; [5]Diagnostic Imaging, Department of Diagnostic Radiology, Fundación Universitaria de Ciencias de la Salud, Hospital Infantil Universitario de San José, Bogotá, Colombia; [6]Neuroradiology, Department of Diagnostic Radiology, Instituto Nacional de Ciencias Médicas y Nutrición, Tlalpan, Ciudad de México, Mexico; [7]IMAGINE, Systems and Computing Engineering, Universidad de los Andes, Bogotá; [8]ImExHS, Imex-Research, Bogotá; [9]Department of Neurological Surgery, Clínica Los Nogales, Bogotá; and [10]Department of Neurology, Fundación Universitaria de Ciencias de la Salud, Hospital Infantil Universitario de San José, Bogotá, Colombia

To whom correspondence should be addressed: Edgar G. Ordóñez-Rubiano, M.D. [E-mail: egordonez@fucsalud.edu.co]

Citation: World Neurosurg. (2019).
https://doi.org/10.1016/j.wneu.2019.01.163

*Journal homepage: **www.journals.elsevier.com/world-neurosurgery***

*Available online: **www.sciencedirect.com***

1 month after resection. The mean follow-up time was 7 months (range, 4–12 months). Residual tumors were treated with radiation and/or with chemotherapy as indicated in an outpatient setting.

CONCLUSIONS: **We present a safe and efficacious preoperative DTI language reconstruction algorithm that could be used as a feasible treatment strategy in a challenging subset of tumors in low- to middle-income countries.**

INTRODUCTION

Many modalities are available to help with preoperative and intraoperative identification of eloquent cortical and subcortical areas. These modalities include diffusion tensor imaging (DTI), DTI-based tractography, functional magnetic resonance imaging (fMRI), direct cortical stimulation (DCS), and direct subcortical stimulation (DSS), motor evoked potentials and sensorial evoked potentials, transcranial magnetic stimulation, and intraoperative magnetic resonance imaging (MRI).[1-3] The development of tractography has provided useful information that can be used to optimize surgical planning and help avoid injury during subcortical dissection of language tracts.[4] In past decades, advancements in neuroimaging technology have made it possible to noninvasively probe the structural and functional connectivity of the cerebrum and derive the Human Connectome Project.[5] DTI provides three-dimensional (3D) anatomic information regarding spatial relationships of subcortical connectivity between essential eloquent cortices.[1] However, given that DSS provides real-time information regarding functional and anatomic features of fiber tracts, intraoperative guidance with DSS has not been replaced by other modalities such as preoperative and intraoperative tractography.

There is considerable variability in the cortical representation of language among individuals. Using standard anatomic landmarks, a 4-cm variability has been found with DCS while performing a resection of gliomas.[6] This lack of reliability between radiographic landmarks and cortical functionality predisposes to an increase in the probability of tract injury intraoperatively when electrophysiologic tools mentioned earlier are not used. As a result, it is difficult to predict precisely where vital language areas may be located. Although the central nervous system (CNS) has been shown to have high plasticity potential,[7,8] subcortical fiber tract plasticity is limited.[9] Adequate recognition of language tracts is imperative in surgical planning for intrinsic frontotemporal lesions, which include, but are not limited to, gliomas,[6,9,10] arteriovenous malformations,[11] and cavernous malformations.[12,13] Initial studies with DTI-based tractography had several limitations, including the poor detailing of fiber tracts, fibers tracts ending before contacting the cortex, an inability to solve fiber crossings, excessive false continuity, and the inability to follow specific bundles within fiber tracts.[14-18] Despite these limitations, tractography can be considered useful for verifying the integrity of deviated tracts, for the localization of deviated tracts, and for evaluating surgical risk.[9,19] The development of new tractography algorithms such as diffusion spectrum imaging,[14,17] high-angular resolution diffusion imaging using bootstrap on q-ball reconstruction,[9] and additional probabilistic methods[20,21] has been a massive boon for the preoperative and intraoperative usefulness of tractography. These new modalities have made it possible to follow fiber tracts through crossings by reducing false continuity.[9,18] The availability of these tools remains limited. In our laboratory for neuroimaging visualization and surgical planning, we have developed new algorithms for acquisitions and for processing[22] to address the limitations of DTI-based tractography.

In this study, we propose a novel algorithm for reconstruction of language ventral and dorsal streams with clinically and commercially available software and application of this algorithm with acquisitions with 3-T and 1.5-T scanners. To our knowledge, this is the first algorithm for low- to middle-income countries (LMICs) that describes how to identify preoperative language tracts with tractography for intrinsic frontotemporal diseases. The objective is to provide a safe, timely, and affordable algorithm for DTI language reconstruction in preoperative planning for lesions that are related to the language tracts to minimize postoperative language disability.

METHODS

Patients

We reviewed a prospectively acquired database of patients who underwent image-guided resection of intrinsic frontotemporal lesions compiled from 2015 to 2018, performed by the senior authors. Clinical and neuroimaging data were obtained on right-handed patients with intrinsic left frontotemporal lesions admitted to the Hospital San José and to the Hospital Infantil Universitario de San José, Bogota, Colombia, between January 2015 and January 2018.

Preoperative imaging was reviewed by the primary author (E.O.R.) in each case to evaluate tumor size and location in determining the potential for study inclusion. Confirmation of an intrinsic frontotemporal location required concordant assessment from a dedicated neuroradiologist (J.M.) as well as the senior authors (W.C., H.C., and E.G.O.M.). All lesions were retrospectively confirmed as being close to language tracts. All cases included preoperative and postoperative DTI acquisitions. Fiber tracking, as well as tract compromise, was performed by a dedicated neuroradiologist (J.M.). Tract compromise was classified as destruction, infiltration, displacement, or unremarkable based on tractography reconstruction. The parameters quantified consisted of a decrease in the number of fibers, displacement of tracts, disruption of fibers, and changes in normal anatomy between both hemispheres in each patient.

Before surgery, all patients had been subjected to routine brain computed tomography and MRI scans. The electronic medical records were retrospectively examined for additional relevant preoperative data (e.g., age, gender, presenting symptoms, and neurologic deficits). Tumor volume for the extent of resection assessment was estimated using measurements obtained from MRI in 3D divided by a factor of 2 (A × B × C/2). The extent of resection was classified as gross total resection (100%), subtotal resection (>90%), or partial resection (<90%).

Clinical and neuroimaging data were also obtained from a large prospective program of babies at the Kangaroo Mother Care program in Bogotá, Colombia.[23] These cases are shown as controls for illustration of the main language tracts in subjects without structural abnormalities (the acquisitions for these cases were obtained at approximately 20 years of age). Authorization was requested to our institutional ethics committee. This study has been approved by the Fundación Universitaria de Ciencias de la Salud, Bogota, Colombia institutional review board.

Imaging Acquisition

1.5-T Scanner. A General Electric Signa Excite HDXT (1.5 T [GE Healthcare, Milwaukee, Wisconsin, USA]) was used to obtain the images. The following sequences were acquired for each patient: axial T1-weighted structural/anatomic and axial DTI. Each structural image in T1 has 140 slices (1 mm thick, without GAP (free space), matrix, 320 × 192; repetition time (TR), 650 milliseconds; echo time (TE), 22 milliseconds; field of view [FOV], 22); and acquisition time, 2 minutes and 35 seconds, covering the entire brain volume. For the isometric DTI sequence, a spin echo-planar sequence with 24 directions was used in an axial plane without angulation. Images were obtained from the base from the skull to the vertex. Each axial tensor sequence has 920 images: matrix, 100 × 100; TR, 14,000–17,000; TE, minimum; thickness 2.5; spacing, 0.0; number of excitations, 1; pixel, 2.5; FOV, 250; b value, 1000; acquisition time, 7 minutes.

3-T Scanner. Structural brain images were acquired on a 3-T scanner, with whole-brain, high-resolution T1-weighted magnetization-prepared rapid gradient-echo images acquired in the sagittal plane (TR, 8.52 milliseconds; TE, 4.13 milliseconds; matrix size, 250 × 256 × 160 mm; voxel size, 0.97 × 0.97 × 1 mm; FOV, 74 mm). The two-dimensional (2D) DICOM (Digital Imaging and Communications in Medicine) files of each brain were organized into volumetric 3D files using the MRIcron software package (http://www.mccauslandcenter.sc.edu/mricro/mricron/).

Processing

1.5-T Scanner. A manual tracing of each region of interest (ROI) and the corresponding deterministic fiber tracking was performed with Functool 9.4.04b (General Electric Medical Systems, GE Healthcare, Milwaukee, Wisconsin, USA). Correction of spin echo-planar distortions (scaling + translation + shearing) was applied. Volume rendering was used to overlay streamlines on the anatomic brain image. Functool 9.4.04b is a commercially available software.

3-T Scanner Voxel-Based Morphometry. The structural T1 images were initially processed using the Computational Anatomy Toolbox (CAT12; developed by Christian Gaser, University of Jena) within the SPM12 software package (Wellcome Department of Cognitive Neurology, London, United Kingdom) and MATLAB R2016a, 9.0.0 (MathWorks, Natick, Massachusetts, USA).[24,25] First, all T1-weighted anatomic images were manually reoriented to place the anterior commissure at the origin of the 3D Montreal Neurological Institute space. The images were then segmented into gray matter, white matter, and cerebrospinal fluid.[26] Segmentations were then inspected for their quality and homogeneity was checked with the CAT12 toolbox. One participant was excluded because of inhomogeneity and motion of the anatomic image. Images were normalized to Montreal Neurological Institute space using a diffeomorphic nonlinear registration algorithm (diffeomorphic anatomic registration through exponentiated lie algebra toolbox [DARTEL]).[27] Images were modulated by the Jacobian transformed tissue probability maps (to obtain volume differences in gray matter) and smoothed with a Gaussian kernel of 8 mm full width at half maximum before statistical analyses. All DTI and T1 fusions were preprocessed with FSL (https://fsl.fmrib.ox.ac.uk/fsl/fslwiki), FreeSurfer (https://surfer.nmr.mgh.harvard.edu/), and Camino (http://camino.cs.ucl.ac.uk), which are freely available libraries. After, images were subsequently visualized through Visual Analytics for Brain Data (BRAVIZ) (http://diego0020.github.io/braviz/) (Universidad de los Andes, Bogotá, Colombia).[22] BRAVIZ is both an open-access python library and a system with a graphic user interface that can be used to analyze brain data. Access to BRAVIZ is free.

Reconstruction Algorithm with DTI-Based Tractography

All ROIs were manually seeded and determined by recognition in 2D tensors in the 3 planes. We used a 7.0-T MRI Brain White Matter Atlas for this purpose.[28]

Superior Longitudinal Fasciculus

The average ROI radius is 3.0 mm. For the reconstruction of the superior longitudinal fasciculus (SLF) temporoparietal segment (SLF-tp), a single ROI was used; the average radius is 7 mm and is in the posterior and inferior aspect of the inferior parietal gyrus, close to the supramarginal gyrus.

Arcuate Fasciculus

The average ROI radius used for reconstruction was 4.0 mm. For the reconstruction of the fractional anisotropy, a single ROI was used in the superior aspect of the insula.

Uncinate Fasciculus

The average ROI radius used for reconstruction was 2.0 mm. The ROI was placed in a temporal subcortical point, at the origin of the temporal stem, in the junction of temporal lobe T1 and T2 tracts.

Inferior Fronto-Occipital Fasciculus

We used a 2.0-mm radius ROI for the reconstruction of the inferior fronto-occipital fasciculus (IFOF), placed in a temporal subcortical location at the level of the temporal stem, in the junction of the middle third with its distal third at its most medial segment.

Inferior Longitudinal Fasciculus

We used a 2.0-mm radius ROI located subcortically in the most inferior periventricular temporo-occipital region in the axial plane. It was also possible to make this reconstruction at the level of the

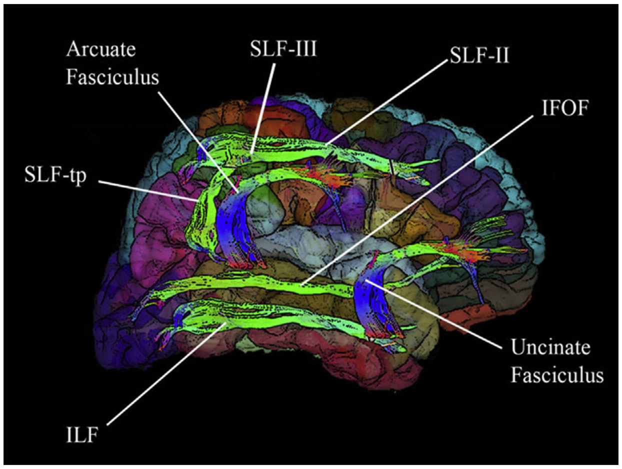

Figure 1. The subcortical anatomy of language. IFOF, inferior fronto-occipital fasciculus; ILF, inferior longitudinal fasciculus; SLF, superior longitudinal fasciculus; SLF-II and III, superior longitudinal fasciculus components II and III; SLF-tp, superior longitudinal fasciculus temporoparietal segment.

temporal stem, in its origin, in the anointing of the tracts of the areas of T4 and T5 of the temporal lobe.

Surgical Procedure

All surgeries were performed by the senior authors (W.C., H.A.C., J.G.P., and E.G.O.M.). A complete imaging protocol was performed, including both preoperative DTI and neuronavigation MRI sequences (T1 or T2 sequences with 1-mm to 2-mm slices without inclination) before each surgical procedure for intraoperative neuronavigation. Surgical resection corridor planning was performed with the neuroradiologist (J.H.M.M.). Trajectories were planned according to preoperative DTI and tractography reconstructions (about 30–60 minutes). All patients were positioned in skull pin fixation for intraoperative neuronavigation (Kolibri [Brainlab, Feldkirchen, Germany] or Aimnav [Micromar Ind. Com. Ltda., Sao Paolo, Brasil]). All surgical supplies and equipment were rented and transferred to our institution the day before surgery, including the neuronavigation system, the physiologic neuromonitoring system (NIM-Eclipse 4 System [Medtronic, Minneapolis, Minnesota, USA]) for brain stimulation, and the ultrasonic aspirator (Sonoca, Söring, Germany). Induction of anesthesia was performed with thiopental or propofol, and an initial neuromuscular block was performed with vecuronium or rocuronium to facilitate intubation as preferred by the anesthesiologist. Anesthesia was maintained with nitrous oxide/oxygen, supplemented by isoflurane and fentanyl or remifentanil in most cases. In general, light surgical anesthesia was maintained, relying on opioid agents to provide adequate analgesia and minimally suppress cortical responsiveness in cases of motor mapping. Subdermal needle electrodes were placed for multichannel electromyographic recording, motor evoked potentials, and sensorial evoked potentials. Skin incision, as well as craniotomy, was performed according to neuronavigation preoperative planning. After dural opening, the cortex was opened where the tumor could be visualized whenever possible. When tumor was not visible at the cortical surface, a minimally invasive transsulcal or transfissural approach was performed. A total en bloc microsurgical resection was performed whenever possible; however, an intralesional resection that used internal debulking of the tumor with an ultrasonic aspirator was performed in most cases. All attempts were made to preserve every cortical and subcortical vein or artery about the tumor. For resection of tumors located near the sensorimotor cortex or subcortical motor tracts, continuous DCS and DSS were performed for mapping around perilesional areas, depending on the cortical/subcortical areas compromised. The construction of the surgical corridor according to the planned trajectory to the tumor, the dissection of fibers, and preservation of language tracts were performed using the preoperative imaging reconstruction algorithm. After resection, the cavity was revised and filled with Surgicel or Floseal if the surgeon considered that resection was subtotal or if there was any risk of postoperative bleeding. Closure was performed in the usual fashion, and the patient was transferred to the intensive care unit for postoperative care.

RESULTS

The language fascicles identified in the patients are summarized in Figure 1. In each patient, we identified the 5 canonic language fascicles described in the literature.[9,29] The seed locations required to derive these fascicles showed a high degree of conformity, with the same location used in all participants. However, fine-tuning of the seed location was required in select instances to reconstruct all fascicles adequately. It was our experience that the arcuate fasciculus (AF) was the most difficult to identify.

A total of 44 cases with tumors were identified in which neuronavigation and preoperative DTI fiber tracking were used for surgical planning. Among these patients, only 10 (7 women, 3 men) aged 28–65 years underwent resection of an intrinsic frontotemporal lesion using preoperative DTI fiber tracking of language tracts. Among these patients, 8 (80%) had high-grade gliomas, and 2 (20%) had cavernous malformations. In 5 patients (50%), the lesion was in the frontal lobe and in 5 (50%), it was in the temporal lobe. Gross total resection was achieved in 5 patients (50%), subtotal resection achieved in 4 (40%) cases, and partial resection in the remaining patient (10%). Compromised tracts included the SLF in 7 (70%), the inferior longitudinal fasciculus (ILF) in 4 (40%), the AF in 3 (30%), and the uncinate fasciculus in 1 (10%). The tracts were infiltrated in 5 patients and displaced in 3 patients. In the remaining patients, the tracts were not compromised, corresponding to the 2 patients with cavernous malformation.

Language function was unchanged or improved in 9 patients (90%). The Karnofsky Performance Status decreased in only 2 of 10 patients (20%), associated with a decline in motor function. New-onset postoperative language decline occurred in only 1

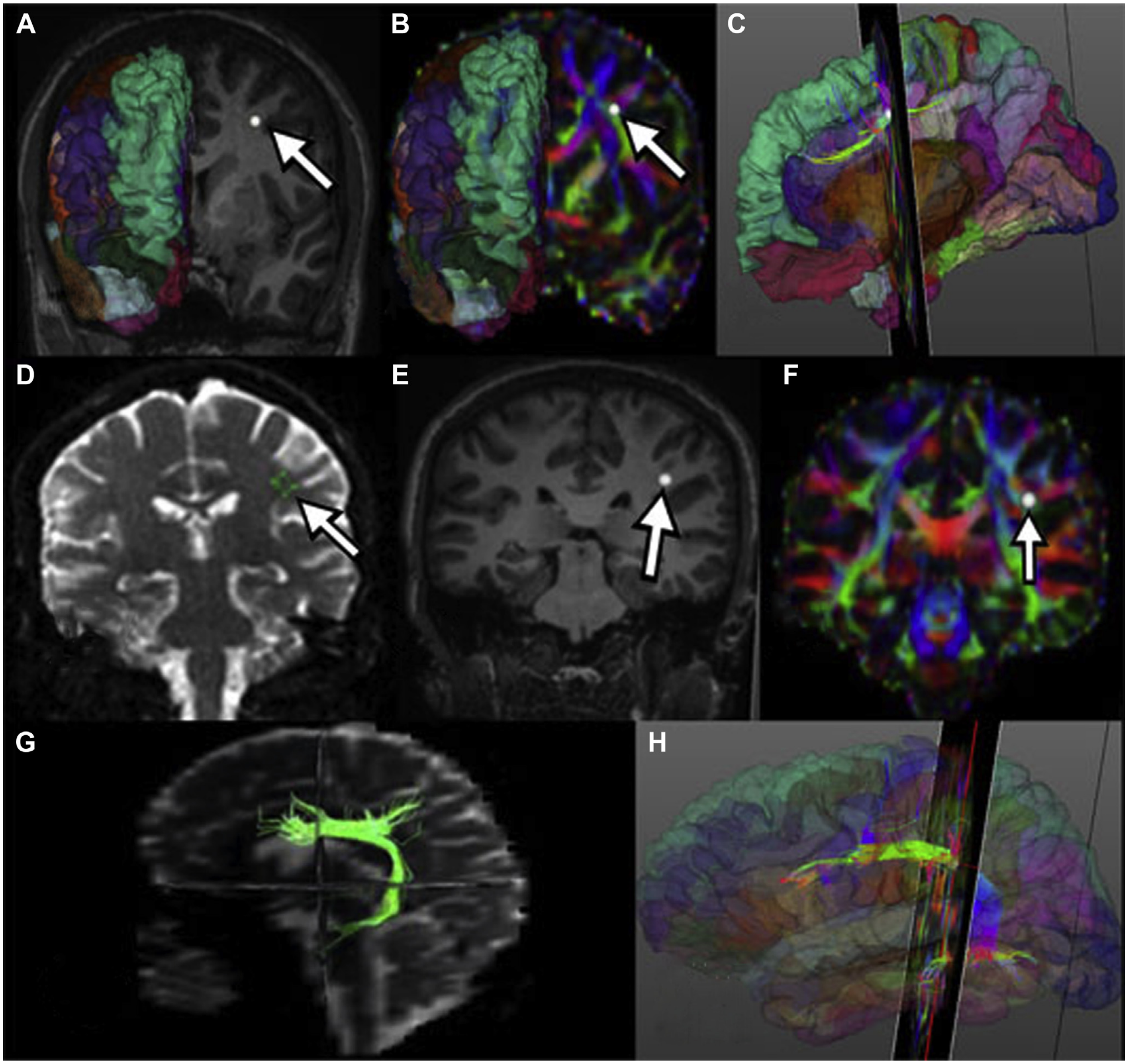

Figure 2. Reconstruction of the superior longitudinal fasciculus (SLF) components II and III (SLF-II/III) and of the arcuate fasciculus. (**A**) Anterior view of the coronal T1 plane is used to show the region of interest (ROI) location (*arrow*). (**B**) The ROI is placed in the coronal fractional anisotropy (FA) color map in the superior and lateral aspect of the corona radiata (*arrow*), (**C**) lateral view of tractography of the SLF-II/III, avoiding arcuate fasciculus as well as other contaminating fibers. (**D**–**F**) Images showing the reconstruction of the arcuate fasciculus. Coronal slices of the tensor, T1, and of the fractional anisotropy maps showing the location of the ROI in the superior aspect to the insula (*arrows*). (**G, H**) 1.5-T and 3-T reconstructions of the arcuate fasciculus.

patient (10%), who recovered transient phonemic paraphasias 1 month after resection. No other complications were reported. The mean follow-up time was 7 months (range, 4–12 months). For high-grade gliomas, residual tumors were treated with radiation and/or with chemotherapy, as indicated by the clinical oncologist in an outpatient setting.

DISCUSSION

SLF

SLF fibers connect frontal lobe structures with surface cortices of the parietal and temporal lobes. However, it is not possible to accurately establish the exact cortical endings of these fibers.

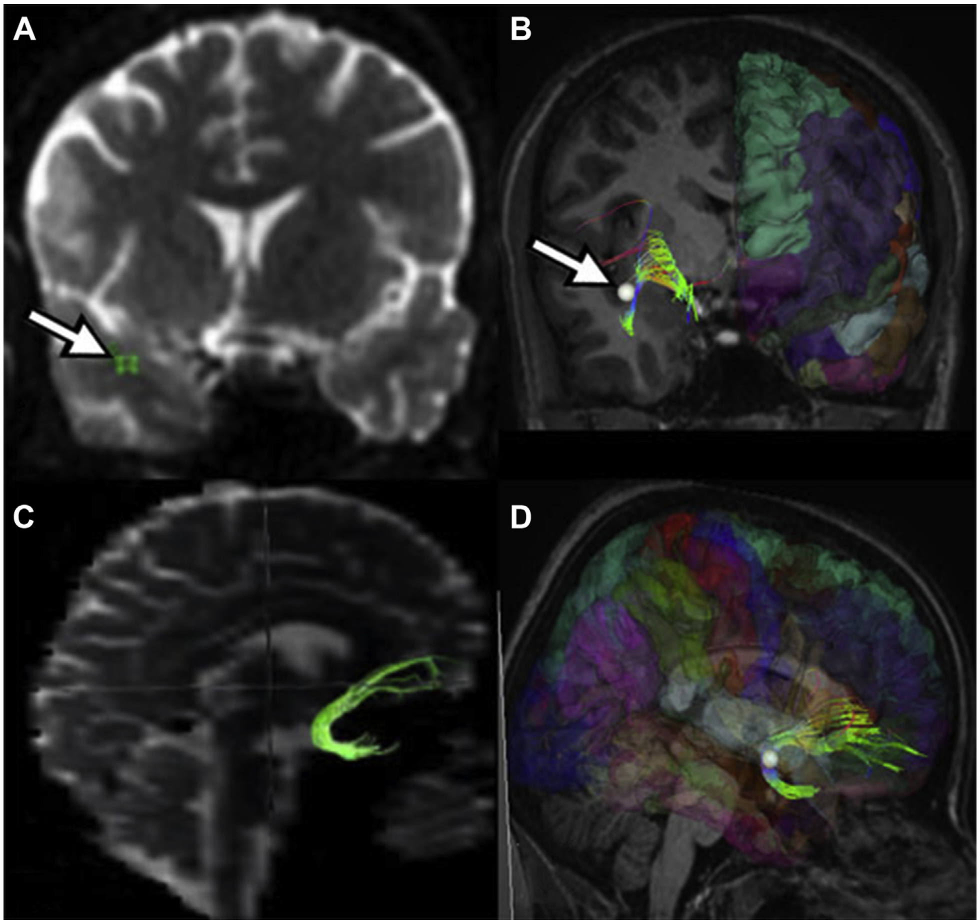

Figure 3. Reconstruction with tractography of the uncinate fasciculus in a healthy individual. The reconstructions were performed with 1.5-T and 3-T scanners. (**A, B**) Coronal sections of the T2 tensor and fractional anisotropy maps, respectively, showing the location of the region of interest at the origin of the right temporal stem, between T1 and T2 subcortical connections (*arrows*). (**C, D**) Isolated three-dimensional reconstruction of the uncinate fasciculus tractography is shown.

There are 5 subsegments of the SLF. The subsegments of the SLF communicate areas of the middle and inferior frontal gyrus with the superior parietal lobe (SLF-I), with the angular gyrus (SLF-II), with the supramarginal gyrus (SLF-III) (also called the operculum-opercular segment), and with the superior and middle temporal gyrus (SLF-tp).[30] The AF has sometimes been included as a component of the SLF. However, some investigators have defined it as an isolated fasciculus,[31] so in our work, we treat it as such because it was separately identified in tractography.

The importance of the SLF lies in its participation in some cognitive functions such as language, work memory, and attention. A study found that SLF lesions can be related to attention-deficit/hyperactivity disorder because of their connectivity with both the frontal and parietal lobes.[29] SLF-I is not significantly involved in language processing[29] and so will not be reconstructed hereafter. The SLF-II originates from the posterolateral region of the parietal cortex from the angular gyrus and terminates in the dorsolateral prefrontal cortex, whereas the SLF-III originates in the supramarginal gyrus and terminates in the ventral premotor and prefrontal cortex.[32] The SLF-tp originates from the posterior part of the superior temporal gyrus and inserts to the posterior portion of the superior parietal gyrus.[32]

Different ROIs have been used for the components of the SLF. Caverzasi et al.[9] recently used multiple ROIs for the reconstruction of the SLF-II, SLF-III, and the AF at the same time: the seed ROI was positioned in the coronal tensor at the level of the isthmus of the corpus callosum, including a region of high anisotropy lateral to the central part of the lateral ventricle and the corona radiata.[33] In addition, these investigators selected different target ROIs: in the angular gyrus for SLF-II, in the supramarginal gyrus for SLF-III, and on the axial peritrigonal plane at the level of the posterior middle and superior temporal gyri for the AF. The ipsilateral frontal lobe was used as a second target ROI. Streamlines that

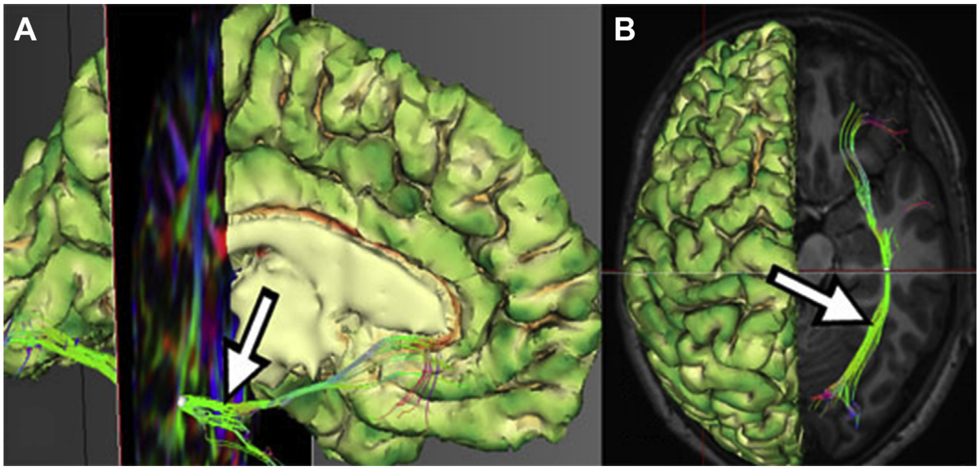

Figure 4. (**A, B**) Three-dimensional reconstruction of the tractography of the inferior fronto-occipital fasciculus (*arrows*) with lateral and superior views, with contralateral brain pial surface reconstruction.

passed through both target ROIs were retained. They also found that the SLF-II and the SLF-III were difficult to separate in some subjects, so they combined these fasciculi into the SLF-II/III for analysis.[9] For reconstruction of the SLF-II and the SLF-III, we used a single ROI in the coronal plane in the lateral aspect of the corona radiata (**Figure 2**).

AF

The subcortical location of the AF is at the frontal region above the upper angle of the insula (**Figure 2**). The AF connects the primary cortical motor and sensorial areas of language (Broca and Wernicke). It has a vital role in the repetition and modulation of language. Its lesion produces conduction aphasia, generating a limitation in the repetition of language, as well as phonemic paraphasias.[31,34]

Uncinate Fasciculus

This white matter structure corresponds to a monosynaptic bidirectional fasciculus, which communicates cortical areas of the anterior superior and middle temporal gyri, and then, it passes through the anterior third of the temporal isthmus, next to the limen of the insula (**Figure 3**). At this point, some of its fibers are mixed with those of the IFOF. It ends at the lateral and medial fronto-orbital area.[4,35] Its function is not accurately understood, but this tract is involved in several cognitive functions such as language, memory, and emotions. The injury of the uncinate fasciculus can lead to alterations in language syntax.[35]

IFOF

Burdachs in 1822[30] was the first to mention a connection between the frontal lobe and the occipital lobe. The frontal-occipital fasciculus has been divided into inferior (IFOF) and superior. However, the existence of the latter is debated. This tract is the longest of the associative fascicles described and connects different areas of the occipital cortex, temporobasal area, and the parietal lobe superior to the frontal lobe.[3] This tract has been identified only in humans.[30] As it enters the frontal lobe, its fibers extend to form a thin dorsolateral curved sheet to terminate in the lower frontal gyrus. The most ventral fibers continue anteriorly and terminate in the orbitofrontal and frontopolar regions (**Figure 4**).[30]

The exact terminations of the IFOF have not been well described. However, a recent study by Carvezasi et al.[36] using a fiber dissection (Q-ball residual bootstrap and using high-resolution high-angular resolution diffusion tractography reconstruction) in 20 healthy individuals found that the tracts were longer than originally described; the IFOF frontal terminations are organized into 4 groups: 1) orbitofrontal region (lateral and middle); 2), inferior frontal (pars orbitalis: Brodmann area 47 and triangularis: area 45 and 3) and ventromedial frontal region (areas 10 and 46); and 4) upper frontal rotation (areas 9 and 10).[3] On the other hand, the posterior terminations of the IFOF include lingual, to the calcarine fissure, the lateral occipital cortex, the angular gyrus, the superior parietal gyrus, the cuneus, and the caudal portion of the fusiform gyrus. The anatomy of the occipital projection pathways is consistent in more than 75% of people.[3]

The role of the IFOF has been linked with attention, visual processing, and language.[2,30] Through intraoperative DSS, it has been documented that this fasciculus is essential in the subcortical network of the semantic system. Therefore, it has been proposed that this fascicle in the dominant hemisphere must be preserved in surgery as much as possible to avoid permanent language impairments.[32,36]

ILF

This fasciculus is responsible for interconnecting temporal and occipital regions, passing parallel to the temporal horn of the lateral ventricle.[37] The ILF, the uncinate fascicle, and the inferior frontal lobe can also play an essential role in the semantic function (**Figure 5**). Some data generate controversy as to when to dissect

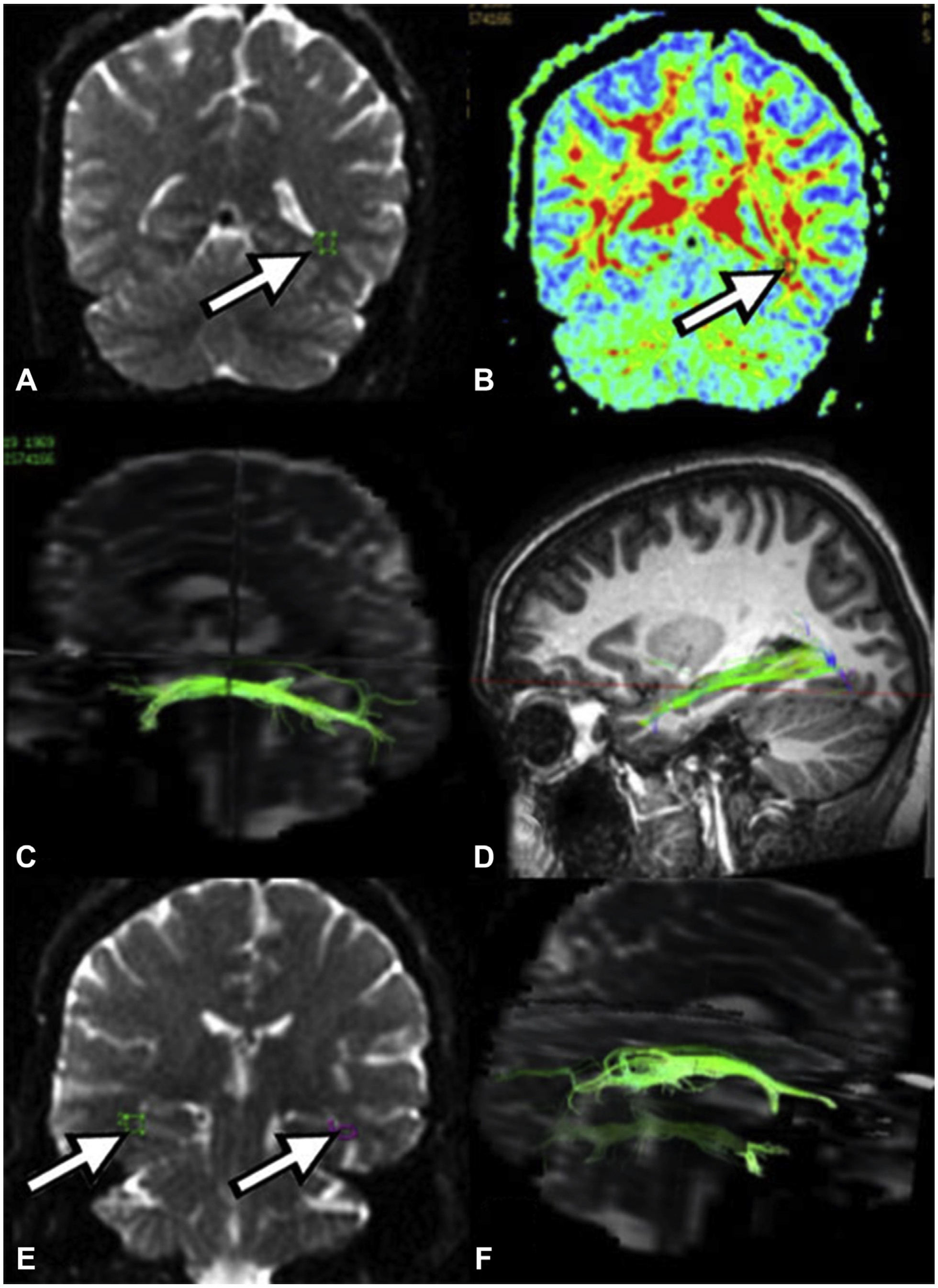

Figure 5. Reconstruction with tractography of the inferior longitudinal fasciculus. (**A, B**) Coronal planes of the tensor and the fractional anisotropy map showing the region of interest at the temporal stem are observed in their origin in the junction of the tracts of the T4 and T5 areas of the temporal lobe (*arrows*). (**C, D**) Three-dimensional reconstruction with 1.5-T and 3-T tractography. (**E, F**) Bilateral regions of interest (*arrows*) in the coronal tensor and bilateral three-dimensional reconstruction of the inferior longitudinal fasciculus.

the ILF and its impact on language. One study showed that removing the ILF surgically leads to deficits in facial recognition,[38] whereas another has shown that the anterior part is involved in linking object representations to their lexical labels.[39]

Illustrative Cases

Case 1. A 56-year-old man presented with paraphasias and seizures. Preoperative MRI showing a left temporal intra-axial lesion, with heterogeneous enhancement, most likely consistent with a

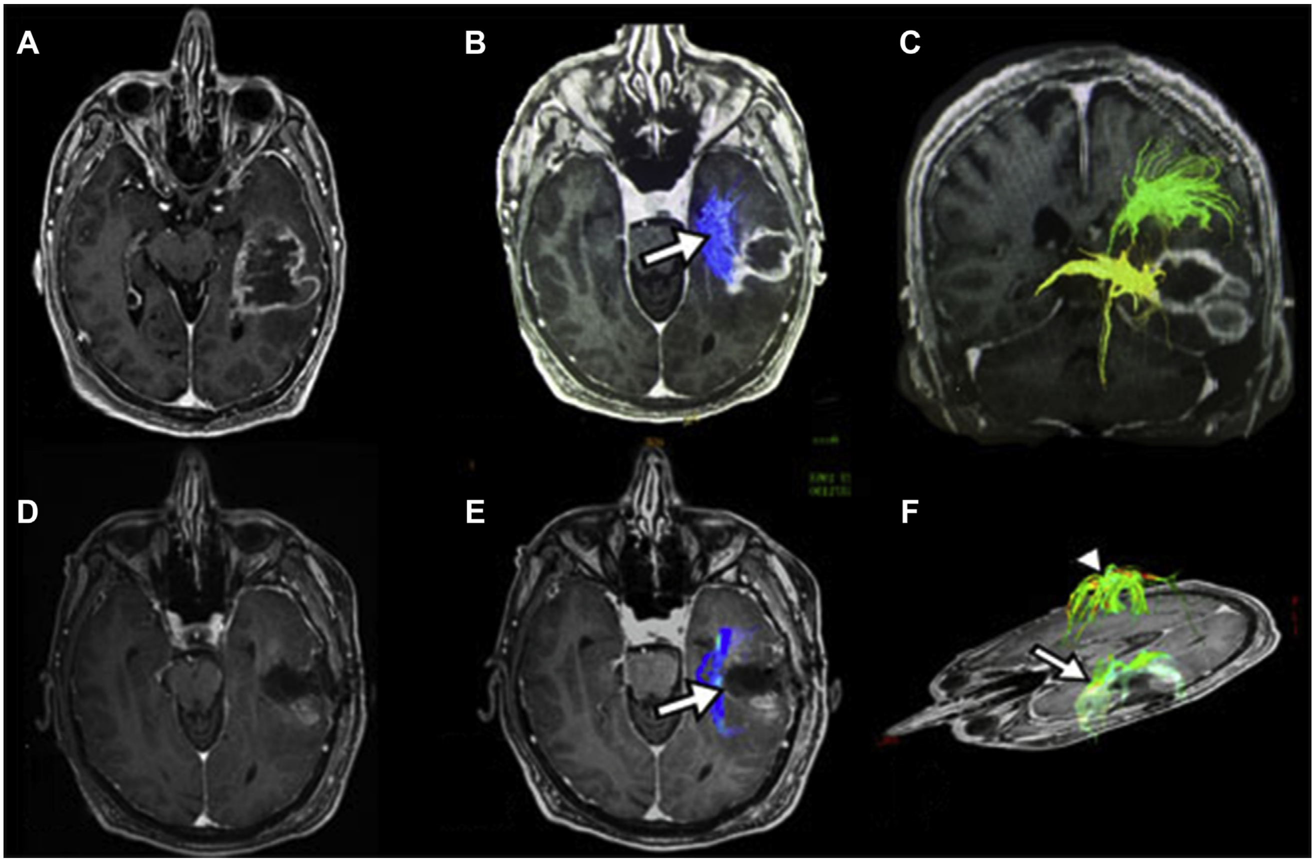

Figure 6. Magnetic resonance imaging of the brain in a patient with a left temporal glioblastoma. (**A**) Axial enhanced T1 showing irregular rim enhancing with central necrosis, suitable for high-grade glioma. (**B**) Tractography in the same patient showing medial displacement of the inferior longitudinal fasciculus (*arrow*). (**C**) Coronal postcontrast T1 showing yellow fibers of the inferior longitudinal fasciculus and green fibers of the superior longitudinal fasciculus. (**D**) Postoperative enhanced magnetic resonance imaging of the head showing near gross total resection of the tumor (**E**), with a decreased number of fibers of the inferior longitudinal fasciculus, with some preserved medial fibers (*arrow*). (**F**) In general preservation of fibers of the inferior (*arrow*) and superior (*arrowhead*) longitudinal fasciculi is observed.

glioblastoma (Figure 6). Medial displacement of language fascicles was noted in the preoperative tractography. A left temporal straightforward approach was performed, achieving a safe near total resection (>90%). No postoperative deficit was noted. The patient recovered from paraphasias and had no recurrent seizures.

Case 2. A 60-year-old man presented to the emergency department with memory loss and generalized seizures. Preoperative enhanced MRI showed a left temporal heterogenous enhancing lesion, with mass effect and displacement of language fibers. Based on preoperative inward and upward displacement of the fibers, a direct transcortical approach was performed, achieving a near total resection, with preservation of the language tracts after surgery (Figure 7). No postoperative deficits were reported, and adequate seizure control was achieved.

Case 3. A 27-year-old man presented to the emergency department with a 2-year left hemicranial headache, associated with episodes of disorientation. No other relevant findings were noted, and no remarkable antecedents were reported. Neurologic evaluation was unremarkable. Preoperative MRI showed a T2 hypointense, T1 postgadolinium hyperintense heterogeneous lesion consisting of a left medial temporal cavernous malformation. The M1 segment of the middle cerebral artery was located anteriorly to the cavernous malformation. Preoperative tractography showed an adequate corridor through the T1 and T2 gyri (Figure 8). A straightforward transcortical approach was performed for resection. Pathologic results were consistent with cavernous malformation. Transient phonemic paraphasias were noted after surgery, which recovered 1 month after resection.

Training, Social, and Economic Limitations

Significant morbidity is associated with left frontotemporal CNS lesions.[40,41] Mortality as a result of CNS malignant tumors has been reported to be increasing in developing countries such as Colombia and Brazil.[42,43] However, neurosurgeons have to face this reality with a lack of advanced technologies in LMICs. Of the

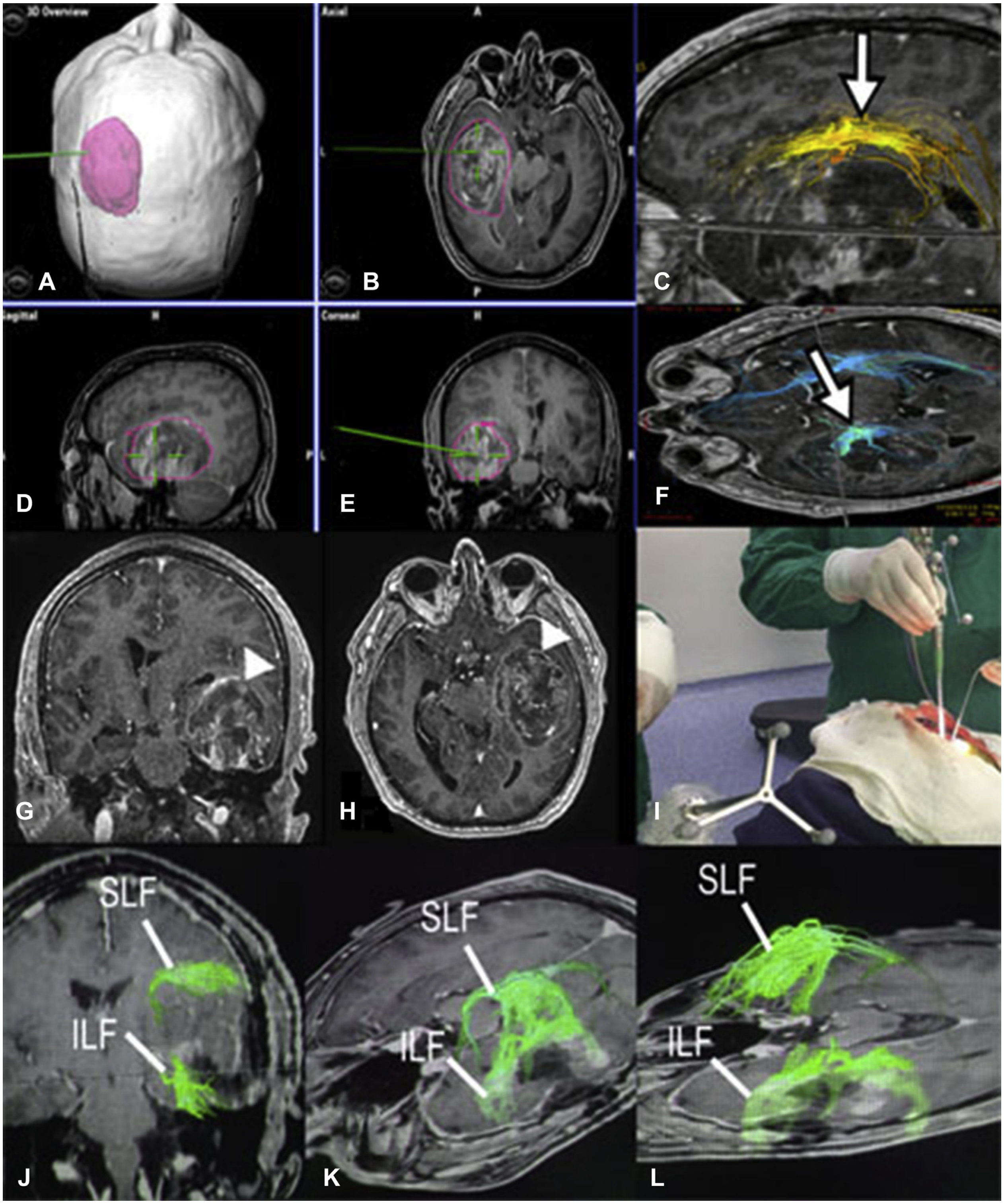

Figure 7. Preoperative enhanced magnetic resonance imaging of the brain in a patient with a left temporal glioblastoma. (**A, B, D, E**) Intraoperative neuronavigation images are shown. Left lateral (**C**) and superior (**F**) views of the tractography showing the superior longitudinal fasciculus (*arrow with yelllow fibers*) superiorly displaced by the tumor and medial displacement of the left inferior longitudinal fasciculus (*arrow with blue fibers*). (**G, H**) Preoperative T1 postcontrast images showing an intrinsic left temporal tumor with heterogeneous enhancement. (**I**) Intraoperative picture of neuronavigation-guided resection. (**J**—**L**) Coronal slice and lateral views of postoperative magnetic resonance imaging showing the three-dimensional reconstruction of the preserved superior and inferior longitudinal fascicles. ILF, inferior longitudinal fascicle; SLF, superior longitudinal fascicle.

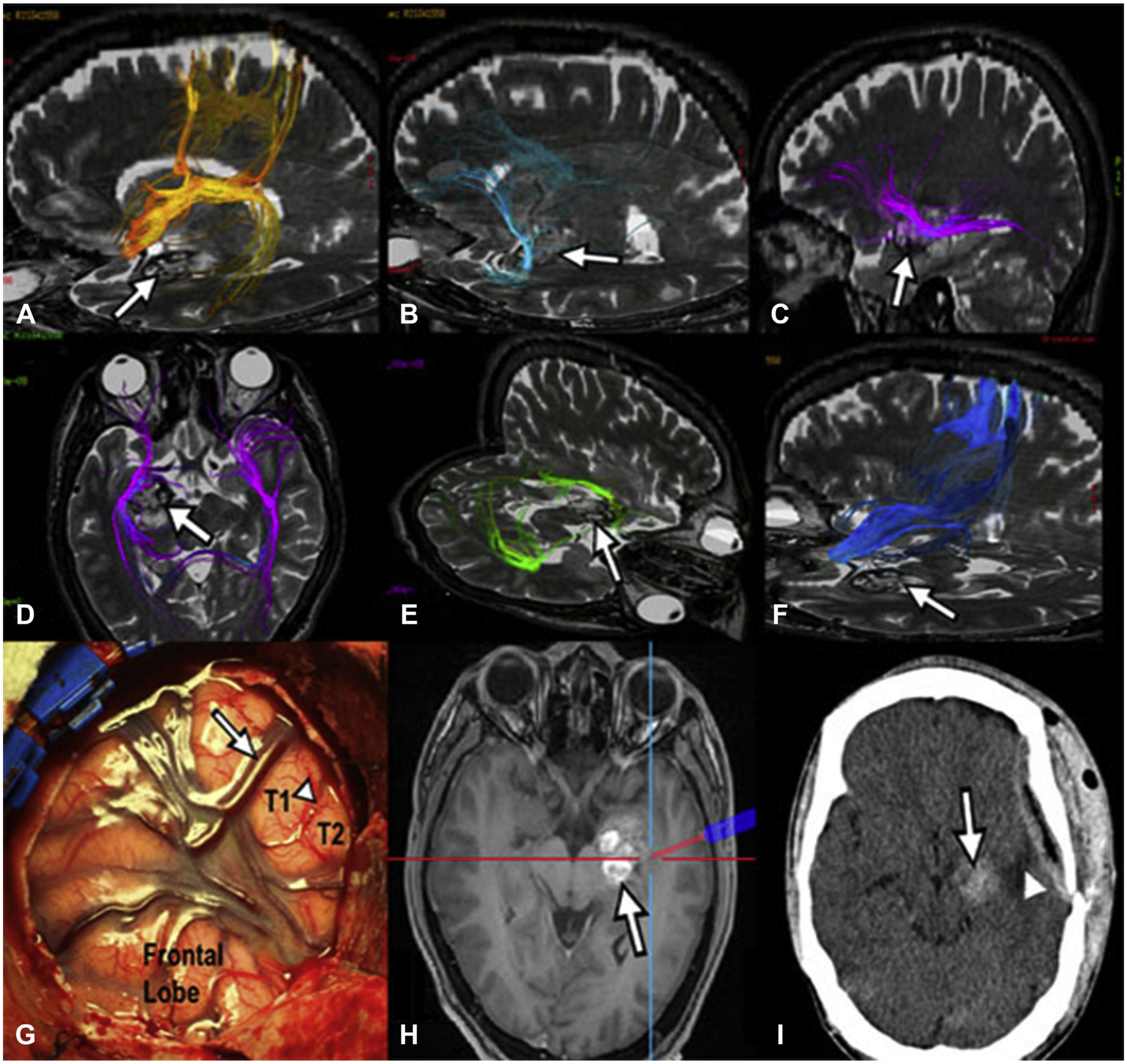

Figure 8. Preoperative fiber tracking of language tracts in a patient with a mesial temporal cavernous malformation. (**A**) The arcuate fasciculus, (**B**) the uncinate fasciculus, (**C, D**) the inferior fronto-occipital fasciculus, (**E**) the inferior longitudinal fasciculus, and (**F**) the medial longitudinal fasciculus are reconstructed. A left temporal, medial cavernous malformation is observed (*arrows*). (**G**) Surgical transtemporal approach. The superior temporal sulcus (*arrowhead*), as well as the vein of Labbé (*arrow*), are shown. (**H**) Intraoperative neuronavigation axial T1 image. (**I**) Axial postoperative image showing complete resection of the cavernous malformation, with hyperdense images of Floseal in the surgical resection spot, as well as a hypodense, left temporal surgical corridor (*arrowhead*).

population in low-income countries in South Asia and Central, Eastern, and Western Sub-Saharan Africa, 90% lack access to essential surgical services.[44] The lack of attention to intrinsic brain tumors is multifactorial and includes economic, social, and technological issues.[44] Resection of intrinsic frontotemporal diseases requires spacious operating rooms, blood banks, equipment (including a microscope, neuronavigation system, and ultrasonic aspirator), as well as intensive care units. In middle-income countries such as Colombia, where access to computed tomography or MRI is restricted but accessible, the significant limitation is the high costs to access advanced technologies such as processing of tractography or the use of

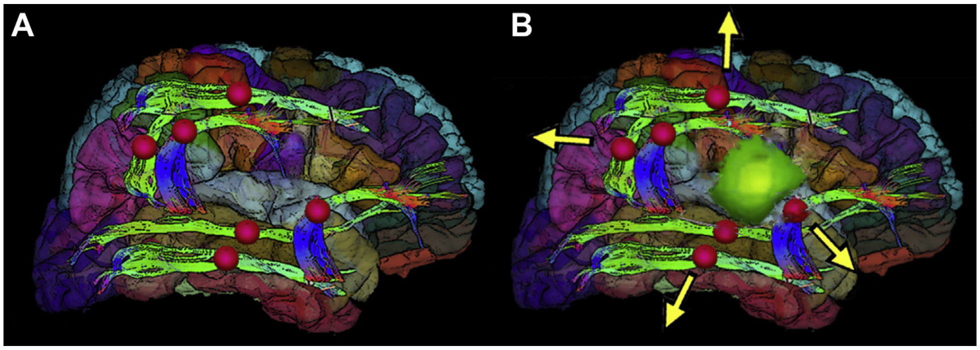

Figure 9. Tractometric points for language tracts. (**A**) A reference illustration showing the tractometric points, marked as red spheres in the middle point of each fasciculus. (**B**) A tumor is represented with a green figure, generating displacement of tracts and the corresponding tractometric points, opening different possible surgical corridors.

neuronavigation systems. Renting surgical supplies and high-tech surgical equipment also represents a considerable limitation to achieving a maximal safe resection.

In most cases, operative resection of intrinsic frontotemporal lesions undergoes surgical treatment but often in suboptimal conditions. In Colombia, costs of renting a neuronavigation system and an ultrasonic aspirator vary between 2000 and 3000 U.S. dollars, and the acquisition and processing of advanced MRI techniques such as fMRI and tractography vary between 300 and 700 U.S. dollars, which includes payment to specialized engineers. In addition, in most public hospitals, there is no MRI scanner. Consequently, MRI scans need to be performed in another facility, which limits adequate communication among technicians, radiologists, and neurosurgeons. Our protocol can be performed not only by engineers or radiologists but also by neurosurgeons or neurosurgery residents without any additional cost. The use of every single tool for these procedures can increase the average cost of the surgery but may lead to cost savings through decreased postoperative morbidity.

Health insurance systems often aim toward reducing upfront medical costs. These institutions may not calculate future cost savings related to more comprehensive prospective treatments. While technology continues to progress, the availability and training of intraoperative DCS are lacking, although they are under development in LMICs. We incorporate this protocol, aiming to simplify tools, including preoperative advanced imaging, which may be available but often neglected by surgeons and which can facilitate maximal safe resection. We present an easy way to reproduce the canonic language tracts with freely available software, using new seeding points for ROIs to identify possible trajectories to intraparenchymal lesions. This surgical planning allows surgeons to identify routes without damaging remarkable white matter tracts. Traditionally, neurosurgeons have been guided through anatomic references or landmarks, starting from craniometric points[45] and entering the brain cortex through cortical/sulcal key points.[46] We introduce in this work the tractometric points for white matter, which could be represented as the middle point of each fasciculus (Figure 9). Displacement of the tractometric points makes a path for surgeons for a safe intraparenchymal corridor.

We firmly believe that intraoperative mapping cannot be substituted with preoperative tractography. However, these images enhance the importance of preoperative planning and may guide surgeons to perform intraoperative cortical and subcortical stimulation according to the preoperative map whenever possible.[47] In addition, interventions associated with intraoperative mapping require skill, experience, and the collaboration of neurosurgeons, specialized nurses, operative room personnel, and adequately trained neuroradiologists, engineers, radiology technicians, anesthesiologists, and neuropsychologists. An incomplete complement of these specialists decreases the chance of achieving the maximal safest resection in these patients.[48,49]

Study Limitations

There are several clinical and technical limitations to this study. First is the small number of patients in whom the tracking was performed. In addition, a multimodal approach (including functional techniques) may explain the occurrence of language deficits more precisely than would a structural connectivity approach.[9] This algorithm for DTI fiber tracking continues to evolve in the process of methodological development. DTI reconstruction is also limited by factors that include poor detailing of fiber tracts, fiber tracts ending before contacting the cortex, an inability to solve fiber crossings, excessive false continuity, and the inability to follow specific bundles within fiber tracts.

In many cases, these limitations may be related to inadequacies referable to the software level. Additional information regarding brain language mapping during awake craniotomies with DSS and resting-state fMRI will address many questions of temporary and permanent declines in the language in these patients, as well as the limitation of brain and tract shifting during surgical resection. Furthermore, this work lacks fractional anisotropy and mean/axial diffusivity analysis and clinical correlation. Preoperative and postoperative neuropsychological evaluation will be a welcome addition to provide more information in the development of further cases. The low- and middle-income economies of developing countries have limited capacity to acquire high technology given its costs, consequently slowing the development of new surgical techniques. Therefore, the design and implementation of our algorithm aim to reduce disparities in brain tumor care in LMICs.

In addition, seeding of the tracts for DTI can introduce variability; there was no control between preoperative and postoperative images and between patients. These reconstructions were based on 2D anatomy in axial tensors. We have not observed considerable differences in anatomic representation between 1.5-T and 3.0-T imaging analysis; however, this mixing represents a significant limitation, making it difficult to draw broad conclusions based on this effort. Although the number of patients examined is insufficient to make more significant observations and insights, this study shows a way to cross barriers and difficulties related to applying this technology in an LMIC.

CONCLUSIONS

We show the successful application of a safe, timely, and affordable DTI tractography reconstruction algorithm to assist in planning for language pathways in intrinsic frontotemporal lesions and in assessing postoperative white matter tract integrity. This algorithm has been successfully implemented at our institution in Colombia, and in this report, we show the feasibility of the implementation of this algorithm in other LMICs.

ACKNOWLEDGMENTS

To doctor Mitchel S. Berger for his guidance and support during the design and execution of this work.

REFERENCES

1. Garrett MC, Pouratian N, Liau LM. Use of language mapping to aid in resection of gliomas in eloquent brain regions. *Neurosurg Clin North Am*. 2012;23:497-506.

2. Sollmann N, Negwer C, Ille S, et al. Feasibility of nTMS-based DTI fiber tracking of language pathways in neurosurgical patients using a fractional anisotropy threshold. *J Neurosci Methods*. 2016;267:45-54.

3. Szelenyi A, Bello L, Duffau H, et al. Intraoperative electrical stimulation in awake craniotomy: methodological aspects of current practice. *Neurosurg Focus*. 2010;28:E7.

4. Fujii M, Maesawa S, Motomura K, et al. Intraoperative subcortical mapping of a language-associated deep frontal tract connecting the superior frontal gyrus to Broca's area in the dominant hemisphere of patients with glioma. *J Neurosurg*. 2015;122:1390-1396.

5. Sporns O, Tononi G, Kotter R. The human connectome: a structural description of the human brain. *PLoS Comput Biol*. 2005;1:e42.

6. Quinones-Hinojosa A, Ojemann SG, Sanai N, Dillon WP, Berger MS. Preoperative correlation of intraoperative cortical mapping with magnetic resonance imaging landmarks to predict localization of the Broca area. *J Neurosurg*. 2003;99:311-318.

7. Teixidor P, Gatignol P, Leroy M, Masuet-Aumatell C, Capelle L, Duffau H. Assessment of verbal working memory before and after surgery for low-grade glioma. *J Neurooncol*. 2007;81:305-313.

8. Moritz-Gasser S, Herbet G, Maldonado IL, Duffau H. Lexical access speed is significantly correlated with the return to professional activities after awake surgery for low-grade gliomas. *J Neurooncol*. 2012;107:633-641.

9. Caverzasi E, Hervey-Jumper SL, Jordan KM, et al. Identifying preoperative language tracts and predicting postoperative functional recovery using HARDI q-ball fiber tractography in patients with gliomas. *J Neurosurg*. 2016;125:33-45.

10. Ulmer JL, Klein AP, Mueller WM, DeYoe EA, Mark LP. Preoperative diffusion tensor imaging: improving neurosurgical outcomes in brain tumor patients. *Neuroimaging Clin North Am*. 2014;24:599-617.

11. Jiao Y, Lin F, Wu J, et al. Brain arteriovenous malformations located in language area: surgical outcomes and risk factors for postoperative language deficits. *World Neurosurg*. 2017;105:478-491.

12. Lin F, Wu J, Wang L, et al. Surgical treatment of cavernous malformations involving the posterior limb of the internal capsule: utility and predictive value of preoperative diffusion tensor imaging. *World Neurosurg*. 2016;88:538-547.

13. Lin Y, Lin F, Kang D, Jiao Y, Cao Y, Wang S. Supratentorial cavernous malformations adjacent to the corticospinal tract: surgical outcomes and predictive value of diffusion tensor imaging findings. *J Neurosurg*. 2018;128:541-552.

14. Alexander DC, Barker GJ. Optimal imaging parameters for fiber-orientation estimation in diffusion MRI. *Neuroimage*. 2005;27:357-367.

15. Duffau H, Gatignol P, Mandonnet E, Peruzzi P, Tzourio-Mazoyer N, Capelle L. New insights into the anatomo-functional connectivity of the semantic system: a study using cortico-subcortical electrostimulations. *Brain*. 2005;128:797-810.

16. Fernandez-Miranda JC, Rhoton AL Jr, Alvarez-Linera J, Kakizawa Y, Choi C, de Oliveira EP. Three-dimensional microsurgical and tractographic anatomy of the white matter of the human brain. *Neurosurgery*. 2008;62(6 suppl 3):989-1026 [discussion: 1026-1028].

17. Wedeen VJ, Hagmann P, Tseng WY, Reese TG, Weisskoff RM. Mapping complex tissue architecture with diffusion spectrum magnetic resonance imaging. *Magn Reson Med*. 2005;54:1377-1386.

18. Fernandez-Miranda JC, Pathak S, Schneider W. High-definition fiber tractography and language. *J Neurosurg*. 2010;113:156-157 [author reply: 157-158].

19. Kikuta K, Takagi Y, Nozaki K, Hashimoto N. Introduction to tractography-guided navigation: using 3-Tesla magnetic resonance tractography in surgery for cerebral arteriovenous malformations. *Acta Neurochir Suppl*. 2008;103:11-14.

20. Berman JI, Chung S, Mukherjee P, Hess CP, Han ET, Henry RG. Probabilistic streamline q-ball tractography using the residual bootstrap. *Neuroimage*. 2008;39:215-222.

21. Bucci M, Mandelli ML, Berman JI, et al. Quantifying diffusion MRI tractography of the corticospinal tract in brain tumors with deterministic and probabilistic methods. *Neuroimage Clin*. 2013;3:361-368.

22. Angulo DA, Schneider C, Oliver JH, Charpak N, Hernandez JT. A multi-facetted visual analytics tool for exploratory analysis of human brain and function datasets. *Front Neuroinform*. 2016;10:36.

23. Charpak N, Ruiz-Pelaez JG, Figueroa de CZ, Charpak Y. Kangaroo mother versus traditional care for newborn infants ≤2000 grams: a randomized, controlled trial. *Pediatrics*. 1997;100:682-688.

24. Ashburner J. Computational anatomy with the SPM software. *Magn Reson Imaging*. 2009;27:1163-1174.

25. Ashburner J, Friston KJ. Voxel-based morphometry—the methods. *Neuroimage*. 2000;11:805-821.

26. Ashburner J, Friston KJ. Unified segmentation. *Neuroimage*. 2005;26:839-851.

27. Ashburner J. A fast diffeomorphic image registration algorithm. *Neuroimage*. 2007;38:95-113.

28. Cho ZH, Calamante F, Chi JG. *7.0 Tesla MRI Brain White Matter Atlas*. 2nd ed. Berlin, Heidelberg: Springer; 2015.

29. Chang EF, Raygor KP, Berger MS. Contemporary model of language organization: an overview for neurosurgeons. *J Neurosurg*. 2015;122:250-261.

30. Bernal B, Altman N. The connectivity of the superior longitudinal fasciculus: a tractography DTI study. *Magn Reson Imaging*. 2010;28:217-225.

31. Basser PJ, Pierpaoli C. Microstructural and physiological features of tissues elucidated by

quantitative-diffusion-tensor MRI. *J Magn Reson*. 2011;213:560-570.

32. Kamali A, Flanders AE, Brody J, Hunter JV, Hasan KM. Tracing superior longitudinal fasciculus connectivity in the human brain using high resolution diffusion tensor tractography. *Brain Struct Funct*. 2014;219:269-281.

33. Mandelli ML, Berger MS, Bucci M, Berman JI, Amirbekian B, Henry RG. Quantifying accuracy and precision of diffusion MR tractography of the corticospinal tract in brain tumors. *J Neurosurg*. 2014;121:349-358.

34. Yamada K, Sakai K, Akazawa K, Yuen S, Nishimura T. MR tractography: a review of its clinical applications. *Magn Reson Med Sci*. 2009;8:165-174.

35. Catani M, Mesulam M. What is a disconnection syndrome? *Cortex*. 2008;44:911-913.

36. Caverzasi E, Papinutto N, Amirbekian B, Berger MS, Henry RG. Q-ball of inferior fronto-occipital fasciculus and beyond. *PLoS One*. 2014;9:e100274.

37. Kiuchi K, Morikawa M, Taoka T, et al. White matter changes in dementia with Lewy bodies and Alzheimer's disease: a tractography-based study. *J Psychiatr Res*. 2011;45:1095-1100.

38. Philippi CL, Mehta S, Grabowski T, Adolphs R, Rudrauf D. Damage to association fiber tracts impairs recognition of the facial expression of emotion. *J Neurosci*. 2009;29:15089-15099.

39. Catani M, Mesulam M. The arcuate fasciculus and the disconnection theme in language and aphasia: history and current state. *Cortex*. 2008;44:953-961.

40. Behin A, Hoang-Xuan K, Carpentier AF, Delattre JY. Primary brain tumours in adults. *Lancet*. 2003;361:323-331.

41. Pineros M, Sierra MS, Izarzugaza MI, Forman D. Descriptive epidemiology of brain and central nervous system cancers in Central and South America. *Cancer Epidemiol*. 2016;44(suppl 1):S141-S149.

42. Monteiro GT, Koifman S. [Brain tumors mortality in Brazil, 1980-1998]. *Cad Saude Publica*. 2003;19:1139-1151 [in Portuguese].

43. Pineros M, Gamboa O, Hernandez-Suarez G, Pardo C, Bray F. Patterns and trends in cancer mortality in Colombia 1984-2008. *Cancer Epidemiol*. 2013;37:233-239.

44. Servadei F, Rossini Z, Nicolosi F, Morselli C, Park KB. The role of neurosurgery in countries with limited facilities: facts and challenges. *World Neurosurg*. 2018;112:315-321.

45. Cotton F, Rozzi FR, Vallee B, et al. Cranial sutures and craniometric points detected on MRI. *Surg Radiol Anat*. 2005;27:64-70.

46. Ribas GC, Yasuda A, Ribas EC, Nishikuni K, Rodrigues AJ Jr. Surgical anatomy of microneurosurgical sulcal key points. *Neurosurgery*. 2006;59(4 suppl 2):ONS177-ONS210 [discussion: ONS210-211].

47. Henry RG, Berman JI, Nagarajan SS, Mukherjee P, Berger MS. Subcortical pathways serving cortical language sites: initial experience with diffusion tensor imaging fiber tracking combined with intraoperative language mapping. *Neuroimage*. 2004;21:616-622.

48. Hervey-Jumper SL, Li J, Lau D, et al. Awake craniotomy to maximize glioma resection: methods and technical nuances over a 27-year period. *J Neurosurg*. 2015;123:325-339.

49. Southwell DG, Hervey-Jumper SL, Perry DW, Berger MS. Intraoperative mapping during repeat awake craniotomy reveals the functional plasticity of adult cortex. *J Neurosurg*. 2016;124:1460-1469.

Conflict of interest statement: The authors declare that the article content was composed in the absence of any commercial or financial relationships that could be construed as a potential conflict of interest.

Received 25 September 2018; accepted 18 January 2019

Citation: World Neurosurg. (2019).
https://doi.org/10.1016/j.wneu.2019.01.163

Journal homepage: ***www.journals.elsevier.com/world-neurosurgery***

Available online: ***www.sciencedirect.com***